Special Collection

Effect of Hyaluronic Acid on the Self-Assembly of a Dipeptide-Based Supramolecular Gel

Bárbara Giménez-Hernández,[a] Eva Falomir,[b] and Beatriu Escuder*[a]

The combination of polymers and low molecular weight (LMW) compounds is a powerful approach to prepare new supramolecular materials. Here we prepare two-component hydrogels made by a well-known and biologically active polymer, hyaluronic acid (**HA**), and a dipeptide-based supramolecular gelator. We undertake a detailed study of materials with different compositions including macroscopic (hydrogel formation, rheology) and micro/nanoscopic characterization (electron microscopy, X-ray powder diffraction). We observe that the two components mutually benefit in the new materials: a minimum amount of **HA** helps to reduce the

polymorphism of the LMW network leading to reproducible hydrogels with improved mechanical properties; the LMW component network holds **HA** without the need for an irreversible covalent crosslinking. These materials have a great potential for biomedical application as, for instance, extracellular matrix mimetics for cell growth. As a proof of concept, we have observed that this material is effective for cell growth in suspension and avoids cell sedimentation even in the presence of competing cell-adhesive surfaces. This may be of interest to advanced cell delivery techniques.

Introduction

Multicomponent supramolecular soft materials are formed by two or more components with functional and/or structural diversity which are blended *via* weak non-covalent interactions. These components may mutually compensate for individual weaknesses along with developing valuable synergies.[1,2] In this context, the combination of low molecular weight gels (LMWG) with polymeric additives may offer a variety of new materials with industrial as well as academic interest.[3,4] LMWG are efficiently produced from molecular components in a few synthetic steps, are monodisperse, and unequivocally pure – and often biocompatible and biodegradable, too. Therefore, materials based on LMWG are unique from the circular economy point of view (atom economy, biodegradability, low waste production, and energy consumption).[5,6] However, many times their mechanical behavior is not optimal – i.e. they are brittle and do not recover their performance after manipulation.

[a] B. Giménez-Hernández, Prof. B. Escuder
Institute of Advanced Materials (INAM)
Universitat Jaume I
12071 Castelló (Spain)
E-mail: escuder@uji.es

[b] Prof. E. Falomir
Departament de Química Inorgànica i Orgànica
Universitat Jaume I
12071 Castelló (Spain)

On the other hand, polymeric soft materials, many of them coming from naturally-based polymers (collagen, polysaccharides), widely exploited for industrial applications, have other associated problems such as polydispersity, batch-to-batch lack of reproducibility or production from animal origin not amenable for certain biomedical applications. Thus, ideally, a careful combination of these two kinds of soft materials could enhance their advantages and moderate their weaknesses. In fact, several groups have shown that polymer additives may influence critical gelation concentration, gelation time, mechanical properties, or even biological activity of LMWGs.[7–17] In this field, different strategies can be used to combine LMWG and polymers. One of them consists of preparing interpenetrating networks (IPNs) in which a second network is formed through the voids of a preformed first network. For instance, Smith et al. reported several examples in which a 1,3:2,4-dibenzylidene sorbitol (DBS)-based LMWG network is combined with alginate or gellan gum as the polymeric component. IPNs were formed in those cases after addition of Ca^{+2} ions as crosslinkers of polymer carboxylate groups.[18,19] This stepwise methodology facilitates the orthogonality of the two networks. In contrast, a second strategy would be to perform the jellification of the two components, LMW compound and polymer, at the same time by the application of heating-cooling cycles or by solvent switch.[9] This procedure allows the interaction of both components during the self-assembly process and may result in either co-assembly or self-sorting of the networks, or even mutual disruption of their self-assembly. A third strategy consists of using soluble polymers which are not able to form hydrogels by themselves. In that case, the polymer acts as an additive that may interact with the LMWG network and modify its physical properties.[13]

Following the last strategy, here we aim to prepare two-component supramolecular gels formed by a dipeptide-based LMWG and a biopolymer. We expect that the polymer additive

ChemBioChem

Research Article
doi.org/10.1002/cbic.202300438

Chemistry
Europe
European Chemical
Societies Publishing

will regulate and enhance the rheological performance of the LMWG component whereas the last will act as a reversible biopolymer crosslinker, minimize the amount of polymer to be used and avoid the need for chemical crosslinking. We have chosen hyaluronic acid (**HA**), a biologically relevant polysaccharide, as the polymer component and *L*-prolyl-*L*-valine dodecylamide (**PVD**) as the low molecular gel counterpart (Figure 1).

PVD is a dipeptide amphiphile previously described in our group based on collagenic amino acid *L*-Pro. **PVD** has been shown to form hydrogels and has been applied in the context of biomimetic organocatalysis.[20,21] However, **PVD**, despite its structural simplicity, has shown a remarkable polymorphism highly dependent on the hydrogel preparation procedures.[22] Firstly, we showed that hydrogels could be obtained by a heating-cooling cycle of a **PVD** suspension. We employed those gels as organocatalysts for direct aldol reactions. However, we soon detected that, randomly, some samples failed to produce a sample-spanning gel network – we initially discarded those for catalytic application. A deeper analysis of all the samples with systematic control of heating temperature and aging revealed, to our surprise, that **PVD** hydrogels and aggregates contained at least three different polymorphs. Moreover, we also investigated the use of pH switching as an alternative methodology for hydrogelation and found an additional polymorph in those gels.[20] Polymorphism was reflected in the size and aspect-ratio of the fibers and, consequently, in the mechanical properties of the hydrogels. Altogether, it resulted in poor reproducibility of the gels.

On the other hand, **HA** is a linear polysaccharide composed of N-acetyl-*D*-glucosamine and *D*-glucuronic acid. **HA** is a widespread component of extracellular matrix and has shown a relevant role in cell signaling, tissue regeneration, and tumor microenvironment, just to mention a few. Moreover, **HA** presents unique properties such as biocompatibility, biodegradability, and non-immunogenicity. Therefore, it is widely used, in different formulations (hydrogels, microemulsions, liposomes), for medical and cosmetic applications, among others.[23] **HA** is omnipresent in the body and the skin concentrates more than 50% of the **HA** content of the body where it has a wide variety of functions, including control of proliferation and differentiation of basal cells and hydration of skin, among others. Therefore, **HA** has found great interest for applications in

transdermal drug delivery, tissue regeneration, and in cosmetics applications such as dermal fillers.[23–25] **HA** is a linear polysaccharide that is not conjugated nor crosslinked in its natural form. However, it is often chemically cross-linked in order to obtain self-sustainable hydrogels for the above-mentioned applications. Recently, examples of supramolecular hydrogels based on **HA** have been reported.[26] In particular, short peptide-**HA** hybrid hydrogels have been introduced as promising materials for biomedical application.[27–30] In addition, the ECM is also formed by a fibrillar network that contains collagens, elastin, fibronectin, and other proteins and glycoproteins.[31] Although the ECM composition depends on the specific tissue, the presence of a fibrillar network is a common trend in all of them. Therefore, ECM mimetics have been fabricated based on naturally occurring polypeptides such as collagen or elastin as well as on synthetic polymers.[32]
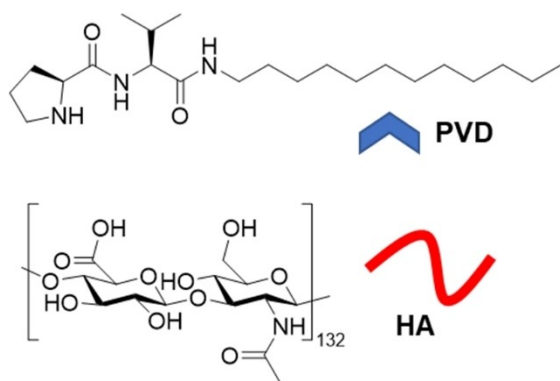
Here we show that a minimum amount of soluble **HA** is sufficient to improve the rheology of **PVD** hydrogels by polymorph selection, favoring the formation of long and thin fibers leading to reversible and reproducible hydrogels. Moreover, this material is effective for cell growth in suspension and avoids cell sedimentation even in the presence of competing cell-adhesive surfaces, which can be of interest for advanced cell delivery techniques.[33]

Results and Discussion

Two-component hydrogel formulation and rheological characterization

In order to modulate the polymorph selection and mechanical properties of **PVD**, we introduced **HA**. Recently, Meijer and co-workers introduced **HA** to obtain benzene-1,2,5-tricarboxamide (BTA)-based supramolecular polymers and hydrogels with tunable stiffness.[34] In that report, the best results were obtained when **HA** was covalently attached to a BTA core and the resulting BTA-**HA** conjugate was able to co-assemble with a BTA-based hydrogelator by means of π–π stacking of the respective aromatic cores. In contrast, the hydrogels formed in the presence of non-conjugated **HA** were much weaker and poorly reproducible as **HA** interfered with the fiber growth leading to the formation of short fibers and increasing polydispersity. However, this case lacks a specific non-covalent interaction between **HA** and the hydrogelator. In our case, we expect that **HA**, which bears one carboxylate group per repeating unit, could establish specific electrostatic interactions with proline ammonium groups of **PVD** during the self-assembly process in water, integrating **HA** at the periphery of **PVD** fibers.

In order to observe the effect of this process, we introduced different amounts of **HA** and we observed the outcome in terms of rheology and fiber morphology. We prepared samples by mixing the required quantities of **PVD** and **HA** (as sodium hyaluronate, 53 kDa) in 4 mL of distilled water, heating until complete dissolution followed by 1 min of sonication and 24 h of stabilization at 25 °C. All the experiments were performed at

Figure 1. Molecular structures and cartoon representation of **PVD** and **HA**.

ChemBioChem

Research Article
doi.org/10.1002/cbic.202300438

**Chemistry
Europe**
European Chemical
Societies Publishing

least in triplicate in order to assess the reproducibility. Results appear collected in Figure 2 and Table 1.

We started by using **PVD** at the minimum gel concentration (mgc), 2 mM. At this concentration, all the samples with different **HA**—COOH mol% going from 0 to 100 (entries 1–5, Figure SI1) led to non-reproducible aggregates and weak gels. Therefore, the experiments were repeated at a higher **PVD** concentration, 4 mM (entries 6–12). In that case, as can be seen in Figure 2, a different outcome was observed. Thus, the addition of equivalent Pro:COOH ratio (100 mol% **HA**—COOH, entry 12) prevented the formation of hydrogels (Figure 2A). On the contrary, the addition of a small amount of **HA**—COOH, as small as 1–5 mol% (entries 7–8), led to homogeneous and reproducible hydrogels (Figure 2E–F) which could be reversibly disassembled and formed after at least three heating-cooling cycles (Figure SI-1). An increasing amount of **HA** (10 mol%, 25 mol%, 50 mol%, entries 9–11) showed a gradual loss of reproducibility in the formation of hydrogels (Figure 2B–D). This trend of hydrogel stability and reproducibility could also be evidenced by rheological studies. Oscillatory rheology experiments were performed on hydrogel samples obtained with different **PVD:HA** ratios (see SI for details). Hydrogels prepared with 2 mM **PVD**, showed G' values in the range of 100 Pa, yield stress values of about 10 Pa and did not recover after rupture for any of the **PVD:HA** compositions, in line with the weak aggregating behavior mentioned before (see Figure SI2). In the case of hydrogels prepared with 4 mM **PVD**, rheology also supports the previous observations (see Figure SI3). As can be seen in Figure 3, samples with 5 mol% **HA**—COOH (entry 7) showed the highest G' values, about 1000 Pa, higher yield stress as well as an 80% recovery after gel rupture. Although G' values are in the same order of magnitude (100–1000 Pa) for all samples in Figure 3, it must be noticed that samples above 10 mol% **HA**—COOH were not reproducible as self-sustained gels. Therefore, G' as well as yield stress values of those samples are not representative of all the replicas. Rheology data should be taken as a tendency, in favor of 1–5 mol% **HA**—COOH samples (entries 7–8) not only because they present slightly higher values but also due to their good reproducibility as self-sustained hydrogels.

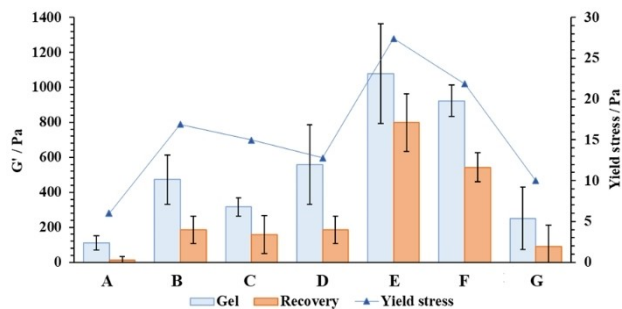## Structural characterization and description of the aggregation mechanisms

In order to rationalize the observed behavior, we must consider the different steps of gel fiber formation and the influence that the presence of an additive such as **HA** may have on them. The formation of hydrogel fibers is based, at molecular level, on the existence of non-covalent intermolecular interactions (van der Waals, hydrogen bonding, etc.) as well as the hydrophobic effect. This self-assembly process can be described as a crystallization from a hot supersaturated solution that involves a primary fibril nucleation step followed by an elongation or fiber growth step. Therefore, starting from a few nucleation centers, aggregates can grow to form long fibers that may entangle and bundle leading to the actual hydrogel fibrillar network.[6]
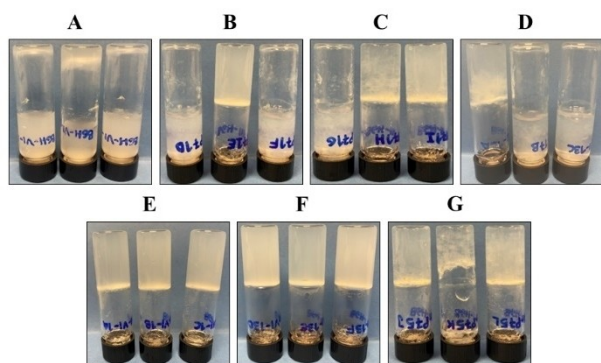
Figure 2. Macroscopic aspect of **PVD** (4 mM) hydrogels prepared with different **HA**—COOH mol%. A) 100; B) 50; C) 25; D) 10; E) 5; F) 1; G) 0.
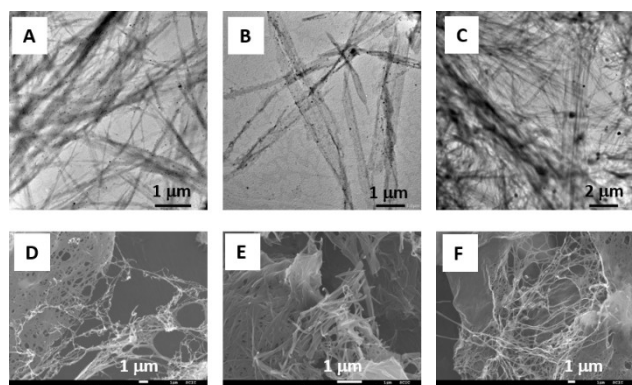
Table 1. Aggregation studies in water.[a]

Entry	PVD (mM)	HA—COOH mol%[b]	Macroscopic aspect[c]	Reproducibility (Y/N)
1	2	0	A – WG	N
2	2	5	A – WG	N
3	2	25	A – WG	N
4	2	50	A – WG	N
5	2	100	A – WG	N
6	4	0	A – G	N
7	4	1	G	Y
8	4	5	G	Y
9	4	10	A – G	N
10	4	25	A – G	N
11	4	50	A – G	N
12	4	100	A	Y

[a] Vial size: 15 mm diameter, 4 mL of distilled water. [b] **HA**—COOH mol% = [(mols **HA**×DP) /mols **PVD**]×100; being DP (degree of polymerization) = 132.
[c] Macroscopic aspect after vial inversion test: G, gel; WG, weak gel; A: non-self-sustaining aggregates.

ChemBioChem

Research Article
doi.org/10.1002/cbic.202300438

**Chemistry
Europe**
European Chemical
Societies Publishing

Figure 3. Oscillatory rheology data of **PVD** (4 mM) hydrogels prepared with different **HA**–COOH mol%. A) 100; B) 50; C) 25; D) 10; E) 5; F) 1; G) 0.
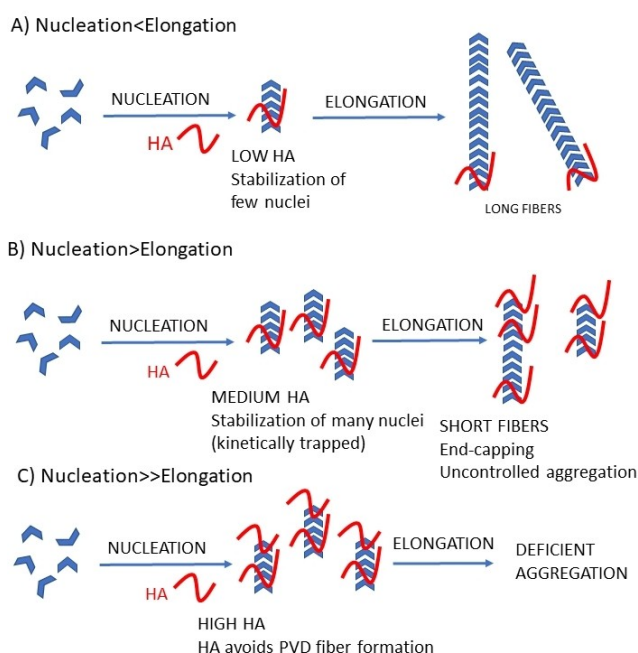
Polymorphism – namely, the adoption of different molecular conformational preferences within the fiber – may affect both nucleation and elongation steps. The presence of different conformations at the nucleation level may cause the seeding of different kinds of fibers. Following the elongation step, it may cause packing mismatches leading to branching or even fiber end capping. Both processes may lead to a deficient network mesh and consequently, to poor mechanical stability. Similarly, the presence of an additive can have either a positive or a detrimental effect on both self-assembly steps.[35] Moreover, the additive can be incorporated as a part of the fiber or not, depending on its solubility and the strength of interaction. In the current case, we are using a short **HA** polymer which is highly soluble in water. Therefore, it will mainly remain in the pools of solvent entrapped by the fibrillar network of **PVD**. To shed light on the morphology and structure of these materials, we performed electron microscopy and X-ray powder diffraction studies. The morphology of the different fibrillar networks was studied by electron microscopy (TEM of fresh hydrogels and SEM of xerogels) (Figure 4). In the case of hydrogels with a 5 mol% of **HA** COOH groups (entry 8), although the presence of drying effects cannot be fully discarded, a uniform distribution of long and thin fibers was observed (Figure 4C and 4F), much regular than in the case of pure **PVD** hydrogels (entry 6, Figure 4A, 4B, 4D, and 4E). Samples with higher content of **HA** showed regions with ill-define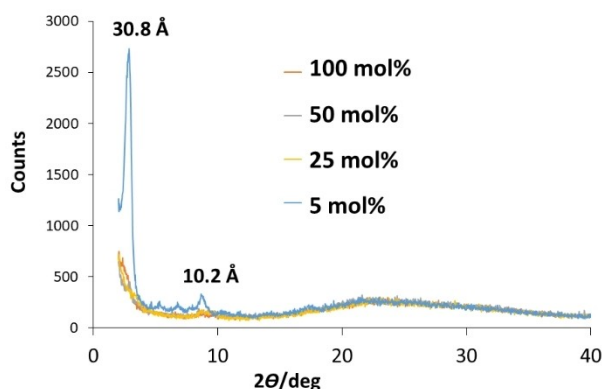d aggregates and, in general, a more heterogeneous aspect (Figure SI4). Materials with >10 mol% **HA**–COOH presented, in general, poor behavior in terms of rheology and morphology as well, calling again to reproducibility issues (entries 9–12). In view of these results, we tried to rationalize the observed behavior and proposed the aggregation mechanism that appears collected in Figure 5. In the case of low **PVD**:**HA** ratio (5 mol% of **HA**–COOH, entry 8), **HA** interacts with the incipient fiber nuclei, protecting them from unspecific agglomeration and favoring the subsequent growth of long and thin fibers and the construction of a homogeneous entangled fibrillar network (Figure 5A). An increase in the amount of **HA** (25–50 mol%, entries 10–11) may increase the number of stabilized nuclei but may also interfere with the fiber growth due to non-specific interactions and changes in viscosity (Figure 5B). Finally, the addition of an equivalent amount of **HA**–COOH (100 mol%, entry 12) completely disrupts the elongation of fibers and leads to a deficient aggregation process (Figure 5C).

Finally, we performed a wide-angle X-ray diffraction analysis of lyophilized xerogels in order to analyze the polymorphic preference for the different compositions (see Figure 6). In the case of high **HA** content samples, no diffraction peaks were detected and only a broad background bump, characteristic of amorphous material, could be observed. However, in the case of 5 mol% samples (entry 8), a clear diffraction pattern was observed which was closely coincident with one of the previously reported polymorphs of **PVD** – in particular, the so-called polymorph D observed when **PVD** hydrogels were obtained by switching from acidic to neutral-basic pH. Polymorph D, as previously reported, corresponds to a molecular packing similar to **PVD** single crystals obtained in acidic media.[22] Therefore, it seems that **HA** is able to stabilize a seminal number of crystallites of protonated **PVD** which act as

Figure 4. Transmission electron micrographs (*top*) and scanning electron micrographs (*bottom*) of samples of pure **PVD** (A, B, D, E) and **PVD** with 5 mol% **HA**–COOH (C, F).

Figure 5. Cartoon representation of the proposed aggregation mechanism for different **PVD**:**HA** COOH molar ratios.

Figure 6. Wide-angle X-ray diffractograms for xerogels of different **PVD**：**HA** compositions.

Figure 7. Optical microscopy images of A-549 cell cultures in the presence of **PVD**：**HA** 5 mol% fibrillar aggregates (A) and in control samples without fibrillar network (magnification 20×).

a template for the growth and elongation of hydrogel fibers. Peaks appear broadened and slightly shifted compared with the pure polymorph D reported before, suggesting the participation of **HA** in these initial nuclei. These results support our initial hypothesis that proposed the electrostatic interaction between **HA** carboxylate and *L*-Pro ammonium groups of **PVD**.

Extracellular Matrix (ECM) mimics for suspended cell growth

As mentioned before, the self-assembled fibrillar networks formed by peptide-based low molecular weight compounds have been identified as candidates for ECM-mimetics. For instance, Ulijn and co-workers showed that short peptide supramolecular hydrogels can be used as a matrix for cell growth.[36] Later on, they also reported that short peptide self-assembled fibers could direct stem cell differentiation depending on hydrogel stiffness.[37] Inspired by these pioneering works, we envisaged that our two-component soft hydrogels could combine the positive effects of a bioactive polymer such as **HA** and a peptide-based supramolecular network. Among all the possible cell-growth experiments, our attention was directed towards suspended cell growth for applications that need to avoid cell sedimentation. One of those is the Convection Enhanced Delivery (CED) of therapeutic cells (for instance, Car T cells) to the brain by intracranial infusion. Sampson and co-workers reported that the injection of the cells suspended into a low-viscosity chemically-crosslinked **HA** hydrogel improved the efficiency of the CED process based on a reduction of the Car T cell sedimentation during the process.[33] Therefore, we tested the ability of our supramolecular hydrogels to both facilitate cell growth and avoid cell adherence/sedimentation. 5 mol% **HA**—COOH hydrogels were prepared into adherent 12-well cell culture treated flat bottom microplates (see SI for details). After hydrogel stabilization, 500 mL of an A-549 cell suspension containing 2×10^5 cells/mL was added over the gels and left in the CO_2 incubator at 37 °C. For control samples, a similar experiment was performed by adding the cell suspension to empty wells. The cultures were followed by observation under the inverted microscope. As can be seen in Figure 7, after
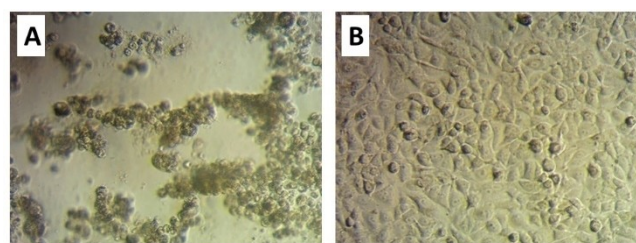
72 h of incubation, a clear difference could be seen between hydrogels and control samples. Hydrogel-containing wells showed bundles of suspended cells surrounding the gel fibrillar network (Figure 7A, see SI for supporting movie) whereas in control samples all the cells were adhered to the bottom of the well (Figure 7B).

Conclusions

In summary, we have reported a new supramolecular multi-component material, fully reversible and non-cytotoxic, with morphological and rheological characteristics that can be modulated exclusively by non-covalent interactions. This material combines a low molecular weight peptide analogue easy to prepare, scalable and cell-compatible, and a well stablished biopolymer, **HA**. Both components are synergistically blended: the polymer component acts as a supramolecular regulator which favours the polymorph selection of **PVD** and, on the other hand, the LMW peptide network acts as a scaffold to harness **HA** within a hydrogel without the need for irreversible covalent crosslinking. It should be mentioned that the amount of **HA** integrated into the hydrogel is in line with the weight % reported for commercial cosmetics and pharmaceutical **HA** formulations. Moreover, as a proof of concept, the as-prepared material has been tested for a specific biomedically relevant application, cell suspension. This behavior may offer opportunities for advanced cell culture and cell delivery techniques.

Experimental Section

Materials. All chemicals and reagents were purchased from commercial sources and used without further purification unless stated otherwise. Sodium hyaluronate (53000 Da) was obtained from the company Polypeptide Therapeutic Solutions (PTS). **PVD** was synthesized according to previously published literature procedures.[20]

Preparation of hydrogels and aggregates. 6.11 mg (0.016 mmols) of **PVD** were weighted in a screwed-capped vial (8 mL, 15 mm of diameter) and the corresponding amount of distilled water or **HA** solution (prepared from dry sodium hyaluronate) was added. Then, the closed vial was heated until complete dissolution, sonicated for 1 minute and stabilized at 25 °C for 24 h prior to being used. Lyophilized samples were prepared by placing the vials containing hydrogels or aggregates in liquid nitrogen for 15 minutes until

ChemBioChem

Research Article
doi.org/10.1002/cbic.202300438

Chemistry Europe
European Chemical
Societies Publishing

completely frozen, followed by lyophilization using a Telstar LyoQuest lyophilizer operating at a temperature of $-86.4\,°C$ and a vacuum of 0.057 mBar.

Oscillatory rheology. Rheological measurements were conducted on a Discovery RH-3 rheometer from TA Instruments using a steel parallel plate-to-plate geometry (40 mm diameter). The gap distance was fixed at 500 μm. The hydrogels were prepared under the desired conditions and incubated for 24 h. Then, hydrogels were deposited onto the rheometer plate and viscoelastic properties were studied under oscillatory experiments. Frequency and strain sweep steps were performed at $23\,°C$. The temperature was controlled strictly using a Peltier system. Each measurement was repeated three times to ensure data reliability. All measurements were conducted within the linear viscoelastic regime (LVR). For this purpose, the experimental conditions to achieve LVR were determined by running a stress sweep (oscillatory stress 0.1–100 Pa at 1 Hz) and a frequency sweep step (0.1–100 Hz at 1 Pa). The storage and loss moduli independence with frequency and oscillatory stress applied defined LVR.

Transmission Electron Microscopy (TEM). Samples (10 μL) were applied directly onto a 200-mesh carbon coated copper grids and were collected directly without staining. TEM images were recorded using a JEOL 1010 Transmission Electron Microscope.

Scanning electron microscopy (SEM). Hydrogel samples were lyophilized, placed on top of an aluminium stub with a carbon sticker and sputtered with Pt. Scanning electron micrographs were taken with a JEOL 7001F microscope equipped with a digital camera.

Wide angle X-ray Diffraction (WAXD). Data collection was performed at room temperature with a BrukerD4 Endeavor X-ray powder diffractometer by using Cu Kα radiation. Xerogels were obtained by freeze-drying and lyophilization. A sample of the xerogel was placed on a sample holder and data were collected for 2θ values between $2°$ and $40°$.

Fourier Transform Infrared Spectroscopy (FT-IR). Spectra were recorded for solid samples using a JASCO FT-IR/6200 spectrometer equipped with an ATR (MIRacle single-reflection ATR diamond/ZnSe) accessory at $4\ cm^{-1}$ ($4000–600\ cm^{-1}$ spectral rangle).

Cell culture experiments. Hydrogels were prepared, following the above-mentioned procedure, under sterile conditions and transferred to 12-well cell culture treated flat bottom microplates. After 24 h, 500 mL of a cellular suspension containing 2×10^5 cells/mL grown in 24-well non-adherent plates (Corning™ Costar™ ultralow adherence microplates) were added on top of the hydrogels (or control samples with no hydrogel) and left into a CO_2 incubator at $37\,°C$. The cultures were followed by observation under the inverted microscope at 10x and 20x magnification for 48, 72, and 96 h. A-549 cells (human lung adenocarcinoma) and DMEM High Glucose supplemented growth medium (FBS 10%, Glutamine 1%, Penicillin/Streptomycin 1% and Amphotericin 1%) were used.

Conflict of Interests

The authors declare no conflict of interest.

Data Availability Statement

The data that support the findings of this study are available from the corresponding author upon reasonable request.

[1] L. E. Buerkle, S. J. Rowan, *Chem. Soc. Rev.* **2012**, *41*, 6089.
[2] J. Raeburn, D. J. Adams, *Chem. Commun.* **2015**, *51*, 5170.
[3] D. J. Cornwell, D. K. Smith, *Mater. Horiz.* **2015**, *2*, 279.
[4] P. R. A. Chivers, D. K. Smith, *Nat. Rev. Mater.* **2019**, *4*, 463.
[5] D. B. Amabilino, D. K. Smith, J. W. Steed, *Chem. Soc. Rev.* **2017**, *46*, 2404.
[6] R. G. Weiss (ed), Molecular Gels: Structure and Dynamics, The Royal Society of Chemistry, **2018**.
[7] X. Y. Liu, P. D. Sawant, W. B. Tan, I. B. M. Noor, C. Pramesti, B. H. Chen, *J. Am. Chem. Soc.* **2002**, *124*, 15055.
[8] Y. J. Adhia, T. H. Schloemer, M. T. Perez, A. J. McNeil, *Soft Matter* **2012**, *8*, 430.
[9] G. Pont, L. Chen, D. G. Spiller, D. J. Adams, *Soft Matter* **2012**, *8*, 7797.
[10] C. Yang, M. Bian, Z. Yang, *Biomater. Sci.* **2014**, *2*, 651.
[11] P. Chakraborty, S. Das, S. Mondal, P. Bairi, A. K. Nandi, *Langmuir* **2016**, *32*, 1871.
[12] P. R. A. Chivers, D. K. Smith, *Chem. Sci.* **2017**, *8*, 7218.
[13] J. Rubio-Magnieto, M. Tena-Solsona, B. Escuder, M. Surin, *RSC Adv.* **2017**, *7*, 9562.
[14] S. L. M. Alexander, L. T. J. Korley, *ACS App. Mater. Inter.* **2018**, *10*, 43040.
[15] R. Das Mahapatra, J. Dey, R. G. Weiss, *Soft Matter* **2019**, *15*, 433.
[16] P. Chakraborty, M. Ghosh, L. Schnaider, N. Adadi, W. Ji, D. Bychenko, T. Dvir, L. Adler-Abramovich, E. Gazit, *Macromol. Rapid Commun.* **2019**, *40*, 1900175.
[17] D. J. Cornwell, D. K. Smith, *Chem. Commun.* **2020**, *56*, 7029.
[18] C. C. Piras, A. G. Kay, P. G. Genever, D. K. Smith, *Chem. Sci.* **2021**, *12*, 3958.
[19] C. C. Piras, P. G. Genever, D. K. Smith, *Mater Adv* **2022**, *3*, 7966.
[20] F. Rodríguez-Llansola, J. F. Miravet, B. Escuder, *Chem. Commun.* **2009**, 7303.
[21] C. Berdugo, J. F. Miravet, B. Escuder, *Chem. Commun.* **2013**, *49*, 10608.
[22] S. Díaz-Oltra, C. Berdugo, J. F. Miravet, B. Escuder, *New J. Chem.* **2015**, *39*, 3785.
[23] J. Zhu, X. Tang, Y. Jia, C.-T. Ho, Q. Huang, *Int. J. Pharm.* **2020**, *578*, 119127.
[24] S. Mitura, A. Sionkowska, A. Jaiswal, *J. Mater. Sci. Mater. Med.* **2020**, *31*, 50.
[25] J. Li, H. Xiang, Q. Zhang, X. Miao, *Pharmaceuticals* **2022**, *15*, 602.
[26] M. Mihajlovic, L. Fermin, K. Ito, C. F. van Nostrum, T. Vermonden, *Multifunct. Mater.* **2021**, *4*, 032001.
[27] M. Aviv, M. Halperin-Sternfeld, I. Grigoriants, L. Buzhansky, I. Mironi-Harpaz, D. Seliktar, S. Einav, Z. Nevo, L. Adler-Abramovich, *ACS App. Mater. Interfaces* **2018**, *10*, 41883.
[28] A. Nadernezhad, L. Forster, F. Netti, L. Adler-Abramovich, J. Teβmar, J. Groll, *Polym. J.* **2020**, *52*, 1007.
[29] J. Rodon Fores, A. Bigo-Simon, D. Wagner, M. Payrastre, C. Damestoy, L. Blandin, F. Boulmedais, J. Kelber, M. Schmutz, M. Rabineau, M. Criado-Gonzalez, P. Schaaf, L. Jierry, *Polymer* **2021**, *13*, 1793.
[30] L. Wang, J. Li, Y. Xiong, Y. Wu, F. Yang, Y. Guo, Z. Chen, L. Gao, W. Deng, *ACS App. Mater. Interfaces* **2021**, *13*, 58329.
[31] N. K. Karamanos, A. D. Theocharis, Z. Piperigkou, D. Manou, A. Passi, S. S. Skandalis, D. H. Vynios, V. Orian-Rousseau, S. Ricard-Blum, C. E. H. Schmelzer, L. Duca, M. Durbeej, N. A. Afratis, L. Troeberg, M. Franchi, V. Masola, M. Onisto, *FEBS J.* **2021**, *288*, 6850.
[32] D. W. Nelson, R. J. Gilbert, *Adv. Health. Mater.* **2021**, *10*, 2101329.
[33] A. F. Atik, C. M. Suryadevara, R. M. Schweller, J. L. West, P. Healy, J. E. Herndon Ii, K. L. Congdon, L. Sanchez-Perez, R. E. McLendon, G. E. Archer, P. Fecci, J. H. Sampson, *J. Clin. Neurosci.* **2018**, *56*, 163.

ChemBioChem

Research Article
doi.org/10.1002/cbic.202300438

Chemistry Europe
European Chemical
Societies Publishing

[34] S. Varela-Aramburu, L. Su, J. Mosquera, G. Morgese, S. M. C. Schoen-makers, R. Cardinaels, A. R. A. Palmans, E. W. Meijer, *Biomacromolecules* **2021**, *22*, 4633.

[35] J.-L. Li, X.-Y. Liu, *Adv. Funct. Mater.* **2010**, *20*, 3196.

[36] V. Jayawarna, M. Ali, T. A. Jowitt, A. F. Miller, A. Saiani, J. E. Gough, R. V. Ulijn, *Adv. Mater.* **2006**, *18*, 611.

[37] E. V. Alakpa, V. Jayawarna, A. Lampel, K. V. Burgess, C. C. West, S. C. J. Bakker, S. Roy, N. Javid, S. Fleming, D. A. Lamprou, J. Yang, A. Miller, A. J. Urquhart, P. W. J. M. Frederix, N. T. Hunt, B. Péault, R. V. Ulijn, M. J. Dalby, *Chem* **2016**, *1*, 298.